Estimate of scattering truncation in the cavity attenuated phase shift PMSSA monitor using the radiative transfer theory

Liu, Fengshan; Snelling, David; Thomson, Kevin; Smallwood, Gregory J.

Publisher's version / Version de l'éditeur:
https://doi.org/10.1080/02786826.2018.1437891
Aerosol Science and Technology, 2018-02-09

Estimate of Scattering Truncation in the Cavity Attenuated Phase Shift PM_{SSA} Monitor Using the Radiative Transfer Theory

Fengshan Liu*, David R. Snelling, Kevin A. Thomson, Gregory J. Smallwood
Measurement Science and Standards, National Research Council
Building M-9, 1200 Montreal Road, Ottawa, Ontario, Canada K1A 0R6

*Corresponding author: Fengshan.liu@nrc-cnrc.gc.ca

Abstract

The recently developed cavity attenuated phase shift particulate matter single scattering albedo (CAPS PM_{SSA}) monitor has been shown to be fairly accurate and robust for real-time aerosol optical properties measurements. The scattering component of the measurement undergoes a truncation error due to the loss of scattered light from the sample tube in both the forward and backward directions. Previous studies estimated the loss of scattered light typically using the Mie theory for spherical particles, assuming particles are present only on the sampling tube centerline, and without accounting for the effects of sampling tube surface reflection. This study overcomes these limitations by solving the radiative transfer equation in an axisymmetric absorbing and scattering medium using the discrete-ordinates method to estimate the scattering truncation error. The present model predicted larger scattering loss than the simplified theoretical estimate in the literature. The effects of absorption coefficient, scattering coefficient, asymmetry parameter of the scattering phase function, and the reflection coefficient at the sampling tube inner surface were investigated. Under typical conditions of CAPS PM_{SSA} operation of low extinction coefficients below about 5000 Mm^{-1}, the scattering loss remains independent of the absorption and scattering coefficients but is dependent on the asymmetry parameter of the scattering phase function and the reflection coefficient of the sampling glass tube inner surface. The scattering loss increases with increasing both the asymmetry parameter and the surface reflection coefficient.

Key words: Aerosol optical properties; radiative transfer equation; scattering loss; cavity attenuated phase shift

1. Introduction

Soot formed during incomplete combustion of fossil fuels mainly consists of carbon. Once emitted into the atmosphere from various combustion devices, soot is generally termed black carbon (BC) particles in the atmospheric sciences and has direct and indirect influences on climate forcing, visibility, and adverse health effects (Bond et al., 2013; Japar et al., 1986; Wilker et al., 2010). Because BC particles have a relatively short lifetime in the atmosphere (on the order of few days to few weeks), it has been suggested that reduction in BC emissions is expected to gain climate and health benefits in a relatively short term (Shindell et al., 2012). To monitor BC mass concentrations from various emission sources, such as on-road vehicles, and in the atmosphere, it is highly desirable to have the real-time measurement capabilities, which can be gained only through optically based techniques.

Optical techniques directly measure the optical properties of aerosols, such as the extinction, scattering, or absorption coefficients, and indirectly yield aerosol mass concentrations with the help of an assumed or known mass absorption coefficient (MAC). Accurate measurement of aerosol light absorption remains a challenge and available techniques for aerosol light absorption measurement have been reviewed by Moosmüller et al. (2009). Extinction-minus-scattering (EMS) techniques remain preferred since they provide more information than other techniques, such as the photoacoustic method. To increase the sensitivity of EMS techniques, aerosol extinction is typically measured by the cavity ring-down (CRD) or the cavity attenuated phase shift (CAPS) techniques and aerosol scattering by a nephelometer (Anderson et al., 1996; Anderson and Ogren, 1998) or an integrating sphere (Varma et al., 2003; Qian et al., 2012; Onasch et al., 2015). It is well known that the truncation issues of nephelometers can give rise to systematic errors in the measured scattering coefficient, which in turn affects the accuracy of the single scattering albedo (SSA) and the derived absorption coefficient (Moosmüller and Arnott, 2003; Bond et al., 2009; Qian et al., 2012; Zhao et al., 2014; Onasch et al., 2015).

Recently, a commercial instrument, called the cavity attenuated phase shift particulate matter single scattering albedo (CAPS PM_{SSA}) monitor, has been developed and described by Onasch et al. (2015) to provide accurate and real-time measurements of particle extinction and scattering coefficients and single scattering albedo at 630 nm or another wavelength in the visible spectrum between 450 and 780 nm. The CAPS PM_{SSA} monitor measures the aerosol extinction using CAPS (Kebabian et al., 2008) and also incorporates an integrating sphere to provide a simultaneous measurement of total scattered light using an integrating sphere. Through careful calibration, CAPS PM_{SSA} is capable of providing absolute measurements of the aerosol extinction and scattering, and

therefore absorption coefficients (Onasch et al., 2015). The measured aerosol absorption coefficient can be used to infer the particle mass concentration if an adequate estimate of the aerosol MAC is available (Petzold et al., 2013). The scattering measurement in CAPS PM_{SSA} using an integrating sphere also suffers from the so-called truncation issues (Onasch et al., 2015), i.e., a certain portion of the scattered light in the forward and backward openings of the sampling tube cannot be collected by the integrating sphere due to geometric constraints. The truncation errors also occur in other nephelometers (Moosmüller and Arnott, 2003; Bond et al., 2009; Zhao et al., 2014). Besides the dimensions of the sampling tube and the integrating sphere, the loss of the scattered light is strongly dependent on the scattering phase function, which is in turn dependent on the wavelength and the size and morphology of the particles. The theories developed so far in the aerosol science community to evaluate the truncation loss have been based on simple considerations of the nephelometer geometry and the scattering phase function of spherical particles from the Mie theory (Moosmüller and Arnott, 2003; Bond et al., 2009; Qian et al., 2012; Zhao et al., 2014; Onasch et al., 2015), rather than by solving the radiative transfer equation (RTE) in an absorbing and scattering medium subject to appropriate boundary conditions. The main drawbacks of these theories lie in the following two aspects. First, aerosol particles are assumed to be spherical and present only along the sampling tube centerline. Second, these simplified methods are unable to take into account the role of reflection on the surfaces of glass sampling tube to the truncation error estimate. Unlike the simple theories developed in the literature above mentioned, the RTE approach is able to account for non-spherical shape of aerosol particles, such as the fractal-like BC particles, and the interactions among aerosol particles present in the entire sampling tube, as well as to account for the effect of the boundary reflection at the sampling tube inner surface. It should be pointed out that in reality reflection occurs at both the inner and outer surfaces of the glass tube. As a simplification, the reflection is assumed to take place only at the inner surface of the glass tube in this study and the reflection coefficient should be treated as an effective one.

In this study, the truncation issue in the CAPS PM_{SSA} monitor was dealt with by solving the RTE in an absorbing and scattering (non-emitting) medium in axisymmetric cylindrical coordinates using the discrete-ordinates method (DOM) to demonstrate the capabilities of the RTE approach in aerosol measurement applications. The effects of the radiative properties of the aerosol particles, in particular the asymmetry factor, and the reflection coefficient of the sampling tube surface on the truncation of scattering measurements are also investigated.

2. The Truncation Issue in CAPS PM_{SSA}

A detailed description of the CAPS PM_{SSA} monitor has been provided by Onasch et al. (2015). A schematic of the monitor is shown in Fig. 1, which is adopted from Onasch et al. (2015).

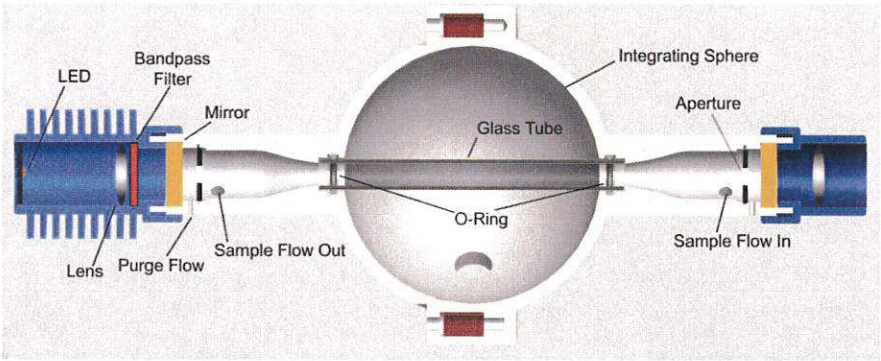

Figure 1. Schematic of the CAPS PM_{SSA} particle single scattering albedo monitor (taken from Onasch et al. (2015)).

This monitor is similar to that used in CAPS PM_{EX} particulate matter extinction monitor (Massoli et al., 2010). However, a 10 cm inner diameter integrating sphere is introduced to measure the scattered light from the aerosol in the section of the sampling tube enclosed by the integrating sphere, Fig. 1. It is noticed from Fig. 1 that the two end sections contain inlets of 7 mm apertures for a gas purge to prevent aerosol particles from depositing on the two end mirrors. The aerosol particles in the sampling glass tube are illuminated by a focused light beam originating from the LED light source. A bandpass filter is used to limit the light to a wavelength in the visible range between 450 and 780 nm. The majority of the scattered light is collected by the integrating sphere, which is coated with a thermally stable, waterproof Avian D white reflectance coating to provide a Lambertian scattering surface with a 98% efficiency over the wavelength range from the near ultraviolet to the near infrared (Onasch et al., 2015). A photomultiplier tube (PMT) placed at the bottom of the integrating sphere in Fig. 1 records the scattered light. It is evident from Fig. 1 that although the majority of the scattered light is collected by the integrating sphere, a certain portion of the scattered light escapes the integrating sphere from the two opening ends of the sampling glass tube and the small sections not enclosed by the integrating sphere. This loss of the scattered light is commonly called the truncation loss or truncation issue.

The light from the light-emitting diode entering the sampling tube is not well collimated. In practice this problem is minimized by only taking measurements of scattering during the signal decay period when the LED light source is off. Only the nearly collimated portion of the light will undergo multiple reflections between the two cavity mirrors. As such, the light beam can be treated as collimated.

The truncation issue can therefore be considered as a radiative transfer problem in an absorbing, scattering, but non-emitting medium in the sampling glass tube subject to a collimated incident light from one end as shown schematically in Fig. 2. The total length of the sampling glass tube is 2s + L and the internal diameter is d. The middle portion of the tube, with a length L, is enclosed by the integrating sphere. The truncation issue is to calculate the radiative flux of the scattered radiation at the internal surface of the sampling tube enclosed by the integrating sphere between z_1 = s and $z_2 = s + L$, Fig. 2. To account for the insertion of the two 7 mm diameter apertures between the two mirrors in CAPSPM$_{SSA}$ shown in Fig. 1, the collimated light enters the left hand side of the sampling tube, Fig. 2, only in the central part of the sampling tube with a radius of 3.5 mm.

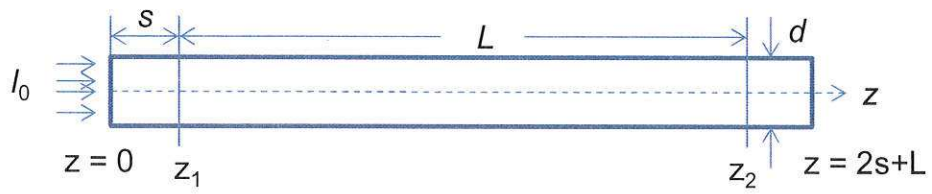

Figure 2. Schematic of the truncation issue in the CAPS PM$_{SSA}$ monitor.

3. Formulation and Solution Method

3.1 Governing equation

For problems with collimated incident radiation, the total spectral radiation intensity field, $I_{t,\lambda}$, can be split into two parts: the scattered field I and the collimated field I_c, i.e., Modest (2013)

$$I_{t,\lambda}(r,z,\Omega) = I_{\lambda}(r,z,\Omega) + I_{c,\lambda}\exp(-\tau_z)\delta(\Omega_c - \Omega) \tag{1}$$

where r, z, and Ω represent the radial position, axial position, and the direction of radiation propagation, respectively. Symbol Ω_c and τ_z are the direction of collimated incidence, which is along the positive z-direction (the centerline of the sampling glass tube shown in Fig. 2), and the optical pathlength at the local position from the boundary of the collimated radiation incidence, respectively. Subscript λ indicates the radiation wavelength. It is noted that the subscript λ is neglected hereafter for simplicity. The scattered radiation intensity field I is governed by the spectral RTE in an absorbing, scattering, and emitting medium in axisymmetric cylindrical coordinates can be written as (Modest 2013)

$$\frac{\mu}{r}\frac{\partial rI}{\partial r} - \frac{1}{r}\frac{\partial \eta I}{\partial \varphi} + \xi\frac{\partial I}{\partial z} = -(k_a + k_s)I + k_a I_b + \frac{k_s}{4\pi}\int_{\Omega'=4\pi} I(\Omega')\Phi(\Omega' \to \Omega)d\Omega' \tag{2}$$

where μ, η, and ξ are the direction cosines along r, φ, and z direction, respectively. Symbols k_a and k_s represent the spectral absorption and scattering coefficient, respectively. Quantity Φ is the scattering phase function that describes the probability of incidence radiation from direction Ω' scattered into

direction Ω. For the truncation problem in aerosol measurements illustrated in Fig. 2, the aerosol medium is normally at the ambient temperature and the blackbody spectral emission term I_b can be neglected.

The following boundary conditions can be assumed. At the two end boundaries of the sampling tube along the z-direction, i.e., at $z = 0$ and $z = 2s+L$, no-reflecting surface is assumed, i.e., the wall emissivity $\varepsilon_w = 1$. This treatment implies that once radiation propagating in the positive z direction (or propagating in the negative z direction) crosses $z = 2s+L$ (or $z = 0$) it will not be reflected back into the sampling tube. At the sampling glass tube inner surface at $r = d/2$, the surface is partially reflecting and partially transmitting with a constant effective reflection coefficient R. Along the tube centerline, the mirror symmetry condition is applied.

3.2 Discrete-ordinates method (DOM)

DOM is used to solve the spectral RTE, Eq. (2), in conjunction with the appropriate boundary conditions discussed above of the problem shown in Fig. 2. For radiative transfer in non-scattering media, DOM in axisymmetric cylindrical coordinates has been described in detail by Liu et al. (2004), which forms the basis of the present numerical method. Following previous studies (Liu et al., 2004; Baek and Kim, 1997), the semi-discrete RTE for radiation intensity along an angular direction defined by a pair of subscript (m, l) can be written as

$$\frac{\mu_{m,l}}{r}\frac{\partial r I_{m,l}}{\partial r} - \frac{1}{r}\left(\frac{\alpha_{m,l+1/2} I_{m,l+1/2} - \alpha_{m,l-1/2} I_{m,l-1/2}}{w_{m,l}}\right) + \xi_{m,l}\frac{\partial I_{m,l}}{\partial z} = -(k_a + k_s) I_{m,l} + S_{m,l} \tag{3}$$

where m is the polar angle index from 1 to M and l is the azimuthal angle index from 1 to $L(m)$. The quantity $w_{m,l}$ is the weight function associated with direction (m, l). The source term $S_{m,l}$ due to in-scattering on the right hand side of Eq. (3) is written as

$$S_{m,l} = \frac{k_s}{4\pi}\sum_{m'=1}^{M}\sum_{l'=1}^{L(m')} I_{m',l'}\Phi_{m',l'\to m,l} w_{m',l'} \tag{4}$$

The solution domain is shown schematically in Fig. 2. The boundary conditions described earlier were implemented in DOM as follows. The outgoing scattered radiation intensities at the two end surfaces of the glass tube are given as

$$\begin{aligned} I_{m,l} &= 0 \quad \text{for } \xi_{m,l} > 0 \quad \text{at } z = 0 \\ I_{m,l} &= 0 \quad \text{for } \xi_{m,l} < 0 \quad \text{at } z = 2s + L \end{aligned} \tag{5}$$

At the tube centerline, the mirror symmetry condition is used

$$I_{m,l} = I_{m,l'}, \quad \text{for } \mu_{m,l} = -\mu_{m,l'} \text{ and } \mu_{m,l} > 0 \tag{6}$$

At the inner surface of the sampling glass tube, a partial reflection condition is used

$$I_{m,l} = R I_{m,l'}, \quad \text{for } \mu_{m,l} = -\mu_{m,l'} \text{ and } \mu_{m,l} < 0 \tag{7}$$

where R is the effective reflection coefficient at the inner surface of the sampling glass tube. It is noticed that the reflection coefficient at a glass surface is in general dependent on wavelength and the incident angle. Although it is relatively straightforward to implement such boundary condition at the inner surface of the glass tube, a simplified boundary condition at the inner surface of the glass tube was considered in this study by assuming an incident angle independent reflection coefficient. It is important to point out that the surface of the sampling tube is assumed to only reflect and transmit, but not absorb, radiation.

3.3 Radiative properties of aerosol particles

The aerosol particles considered in this study are typical combustion generated soot, whose radiative properties can be calculated with reasonably good accuracy using the RDG approximation for fractal aggregates (RDG-FA). The particular version of the RDG-FA approximation used in this work is the same as that described in Liu et al. (2009) for the absorption and total scattering cross sections and the scattering phase function of log-normally distributed polydisperse soot aggregates. In addition, the effects of the aerosol particle radiative properties, namely the absorption and scattering coefficients and the asymmetry parameter on the scattering truncation in the CAPS PM_{SSA} monitor were also investigated. To simplify the numerical integration of the in-scattering term expressed in Eq. (4), the scattering phase function is represented using the single-parameter Henyey-Greenstein approximation given as (Modest 2013)

$$\Phi(\Omega' \rightarrow \Omega) = \frac{1-g^2}{(1+g^2-2g\cos\theta)^{1.5}} \tag{8}$$

where g is the asymmetry parameter ($-1 \le g \le 1$) and θ is the scattering angle evaluated as

$$\cos\theta = \mu\mu' + \eta\eta' + \xi\xi' \tag{9}$$

3.4 Definition of truncation

In this study, the radiative flux integrated over the entire 4π solid angles is used as a measure to quantify the scattering truncation, i.e.,

$$q_i = \int_{4\pi} \zeta_i I d\Omega \tag{10}$$

where ζ_i is the direction cosine for the direction under consideration. The total scattered radiation signal collected by the integration sphere S_{gain} is the integration of q over the glass tube internal surface between $z_1 = s$ and $z_2 = s + L$ shown in Fig. 2. The integration of q over the two planes at $z_1 = s$ and $z_2 = s + L$ is considered as the scattering signal loss, S_{loss}. The truncation is then defined as a ratio $T_s = S_{gain}/(S_{gain}+S_{loss})$. It is believed that this definition is consistent with that implied the expression of

Onasch et al. (2015). Therefore, the present results can be compared to those given in Onasch et al. (2015).

4. Results and Discussion

Unless otherwise stated, the dimensions of the CAPS PM_{SSA} monitor sampling glass tube are used in the present calculations, i.e., $d = 1$ cm, $L = 10$ cm, and $s = 1$ cm based on the publication of Onasch et al. (2015) and the reflection coefficient at the inner surface of the glass tube is set at $R = 0.2$. In this study, the T_6 quadrature in the axisymmetric cylindrical geometry, which consists of 144 angular directions with $M = 42$, was used in all the calculations. Further details of the present DOM implementation follow closely those described in detail in Liu et al. (2004). A uniform grid of 221×31 was used in the z- (along the tube) and r-direction (radial), respectively. Iteration was stopped when the maximum relative variation in the solid angle integrated scattered intensity is less than 5×10^{-3}. The radiative properties of the aerosol particles, namely k_a, k_s, and Φ, in the sampling glass tube of CAPS PM_{SSA} were first considered to be those of typical combustion generated soot and were calculated by the Rayleigh-Debye-Gans (RDG) theory for fractal aggregates (Liu et al., 2009). For primary soot particles of 30 nm in diameter, the absorption and scattering cross sections of the lognormally distributed soot aggregates in the study of Liu et al. (2009) at 630 nm are estimated from those at 400 and 780 nm given in Liu et al. (2009) as $C_a = 1.0\times10^{-14}$ m^2 and $C_s = 0.138\times10^{-14}$ m^2 and the asymmetry parameter is $g = 0.61$.

It is normally required by CAPS PM_{SSA} that the aerosol particle concentrations are sufficiently low to keep the extinction coefficients below about 2000 Mm^{-1} (1 Mm^{-1} = 10^{-6} m^{-1}) to avoid the fouling of the sampling glass tube. The following absorption and scattering coefficients were used to represent the soot generated in the laminar diffusion flame: $k_a = 2000$ Mm^{-1} and $k_s = 276$ Mm^{-1}. Later calculations were conducted by varying k_a, k_s, g, and R to investigate how these parameters affect the truncation. Under the conditions of soot generated in a laminar diffusion flame, the truncation was found to be 0.804, i.e., there is significant scattering loss of about 20%, since the scattering phase function of these soot aggregates is peaked in the forward direction with $g = 0.61$, causing considerable loss of the scattering in the forward directions.

Since the aerosol particles are assumed to be uniformly distributed in the sampling glass tube, it is useful to examine a simple geometrical consideration in the limiting case of isotropic scattering. In this case, the truncation should approach the ratio of the glass tube internal surface area enclosed by the integrating area to the total surface area of section of length L shown in Fig. 2, i.e., T_s = 10/(10+0.35) = 0.9662. The truncation from numerical calculation for $g = 0$ (isotropic scattering) is 0.9678, which is very close to that based on simple geometric reasoning. In addition, an examination

of the calculated radiative fluxes at the two cross sections at $z_1 = s$ and $z_2 = s + L$ indicate that q_{z2} is almost the same as q_{z1} in the case of isotropic scattering, but q_{z2} becomes increasingly larger than q_{z1} with increasing the asymmetry parameter g, as expected. At $g = 0.61$, q_{z2} is about 3 times of q_{z1}.

4.1 Effect of the absorption coefficient

Numerical results for varying the absorption coefficient, while keeping all other parameters constant at k_s = 1000 Mm^{-1}, g = 0.61, and R = 0.2, indicate that the truncation T_s remains almost unchanged at 0.8039 for a wide range of absorption coefficient from 0 to 5000 Mm^{-1}. This is because the absorption coefficient in this range is too small to cause a change in the radiation intensity over one pathlength of the sampling tube (here 12 cm).

4.2 Effect of the scattering coefficient

Numerical results were conducted for a range of k_s between 500 and 3000 Mm^{-1}, while keeping all other parameters constant at k_a = 1000 Mm^{-1}, g = 0.61, and R = 0.2. The results indicate that the truncation T_s again remains unchanged at 0.8039 over the range of k_s considered and the radiative fluxes at the sampling tube surface and at $z_1 = s$ and $z_2 = s + L$ along the tube increase with increasing k_s and are proportional to k_s.

The above results suggest that the truncation under the normal operation conditions of CAPS PM_{SSA} is determined by the scatter phase function (through the asymmetry factor g) and the sampling tube inner surface reflection coefficient R, but independent of the particle concentration, which affects the absorption and scattering coefficients.

4.3 Effect of the asymmetry parameter *g*

The effect of g on the truncation was calculated over a range of g values between 0 (isotropic scattering, which is approximately the case for very small spherical particles in comparison to wavelength) and 0.8 (highly forward scattering), since this range covers essentially the whole range of g encountered in BC measurements from isolated primary particles to large aggregates. The effect of g on truncation is shown in Fig. 3 while keeping other properties constant given in the figure. It is seen that the truncation is about 97% for isotropic scattering, which is very close to the simple geometric reasoning discussed above, and then starts to decrease rapidly with increasing g. This is expected since with increasing g, the scattering phase function is more forward peaked, leading to more scattered radiation loss in the forward direction, i.e., more scattered light escapes from the right hand side of the sampling tube at $z_2 = s + L$ shown in Fig. 2. The decreasing trend of truncation with increasing g, which corresponds to increasing particle size, is in qualitative agreement with the results of Onasch et al. (2015).

To directly compare the results shown in Fig. 3 to those of Onasch et al. (2015), it is necessary to obtain the asymmetry parameter of the polystyrene latex (PSL) particles (m = 1.53 + 0.02i) considered in the study of Onasch et al. (2015). For a PSL particle of 500 nm in diameter at λ = 450 nm, the asymmetry parameter calculated by the Mie theory is g = 0.7581. The present numerical model predicted a truncation of T_s = 0.707 for R = 0.2. On the other hand, the simple model used by Onasch et al. (2015) estimated the truncation to be about 0.92, which is significantly higher than the present result. This comparison implies that the simplified theoretical model used by Onasch et al. (2015) significantly overestimates truncation, i.e., underestimates the loss of scattered signal from the CAPS PM_{SSA} monitor.

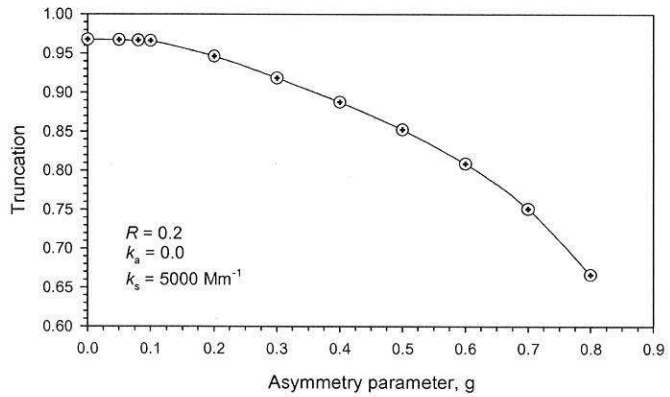

Figure 3. Variation of the truncation with the asymmetry parameter g.

4.4 Effect of the glass tube surface reflection coefficient *R*

The reflection coefficient at the sampling glass tube inner surface is potentially an important parameter to affect the truncation. It is useful to understand how the surface reflection influences the truncation, since the surface condition of the sampling tube may vary over time, such as due to deposition of aerosol particles, which tends to decrease the reflection coefficient. The variation of truncation with the sampling tube surface reflection coefficient is shown in Fig. 4, while keeping other properties constant with the values shown in the figure. The truncation decreases modestly with increasing the surface reflection coefficient from 0 (non-reflecting) to 0.5. These results suggest that the increase in surface reflection coefficient increases the scattered radiation loss from the sampling tube in the forward and backward directions, leading to a decrease in the truncation. This is reasonable based on the considerations that the reflected radiation at the sampling tube surface reduces the scattered radiation entering the integrating sphere and enhances the chance of the scattered radiation escaping the sampling tube in the forward and backward directions through multiple reflections at the sampling tube surface. These results also suggest that it is better to use a low reflection/high transmission material for the sampling tube to reduce the loss of scattered light from CAPS PM_{SSA}.

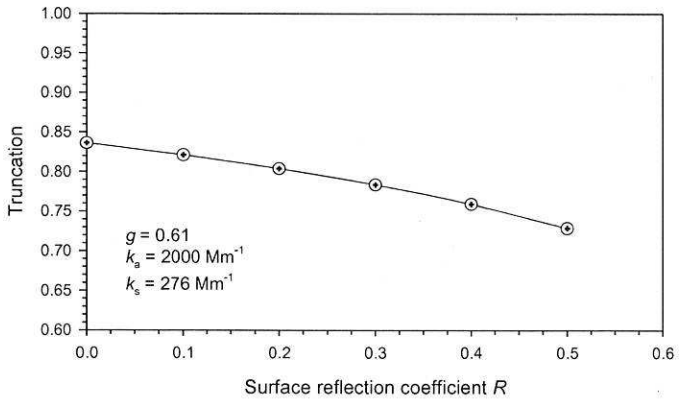

Figure 4. Variation of the truncation with the sampling tube surface reflection coefficient R.

5. Conclusions

A radiative transfer equation based model was employed to predict the loss of scattered radiation in the Aerodyne CAPS PM_{SSA} monitor. The present numerical model is much more capable than the simple theoretical estimate to account for more detailed sampling tube geometry, particle distribution in the sampling tube, and the boundary condition at the inner surface of the sampling glass tube. The present model predicted more significant loss of scattered radiation from this monitor than the simple model proposed in the literature for aerosol particles of a similar asymmetry parameter. The numerical results obtained in this study show that under the normal operation conditions of CAPS PM_{SSA} the truncation is independent of the aerosol absorption and scattering coefficients, i.e., the particle mass concentration, but decreases significantly with increasing the asymmetry parameter, and decreases modestly with increasing the surface reflection coefficient. Therefore, for a given sampling tube the most important parameters affecting the truncation are the aerosol particle asymmetry parameter and the sampling tube surface reflection coefficient. Further research is required to investigate the effect of the integrating sphere size and to implement more realistic boundary condition at the inner surface of the sampling glass tube.

REFERENCES

Anderson et al., 1996; Anderson and Ogren, 1998) or an integrating sphere (Varma et al., 2003; Qian et al., 2012; Onasch et al., 2015)

Anderson, T.L., Covert, D.S., Marshall, S.F., Laucks, M.L., Charlson, R.J., Waggoner, A.P., Ogren, J.A.., Caldow, R., Holm, R.L., Quant, F.R., Sem, G.J., Wiedensohler, A., Ahlquist, N.A., and Bates, T.S. (1996). Performance Characteristics of a High-Sensitivity, Three-Wavelength, Total Scatter/Backscatter Nephelometer. *J. Atmos. Oceanic Technol.*, 13:967-986.

Anderson, T.L., and Ogren, J.A. (1998). Determining Aerosol Radiative Properties Using the TSI 3563 Integrating Nephelomter. Aerosol Sci. Technol. 29:57-69.

Baek, S.W., Kim, M.Y. (1997). Modification of the Discrete-Ordinates Method in an Axisymmetric Cylindrical Geometry, *Num. Heat Transfer, Part B* 31:313-326.

Bond, T.C., Covert, D.S., Müller, T. (2009). Truncation and Angular-Scattering Corrections for Absorbing Aerosol in the TSI 3563 Nephelometer, *Aerosol Sci. Technol.* 43:866-871.

Bond, T.C., Doherty, S.J., Fahey, D.W., Forster, P.M., Bemtsen, T., et al. (2013). Bounding the Role of Black Carbon in the Climate System: A Scientific Assessment, *J. Geophys. Res.: Atmos.* 118:5380-5552.

Japar, S.M., Brachaczek, W.W., Gorse Jr, R.A., Norbeck, J.M., Pierson, W.R. (1986). The Contribution of Elemental Carbon to the Optical Properties of Rural Atmospheric Aerosols, *Atmos. Environ.* 20:1281-1289.

Kebabian, P.L., Wood, E.C., Herndon, S.C., and Freedman, A. (2008). A Practical Alternative to Chemiluminescence-based Detection of Nitrogen Dioxide: Cavity Attenuated Phase Shift Spectroscopy. Environ. Sci. Technol. 42(16):6040-6045.

Liu, F., Guo, H., Smallwood, G.J. (2004). Effects of Radiation Model on the Modeling of a Laminar Coflow Methane/Air Diffusion Flame, *Combust. Flame* 138:136-154.

Liu, F., Thomson, K.A., Smallwood, G.J. (2009). Numerical Investigation of the Effect of Signal Trapping on Soot Measurements Using LII in Laminar Coflow Diffusion Flames, *Appl. Phys. B* 96:671-682.

Massoli, P., Kebabian, P., Onasch, T.B., Hills, F., Freedman, A. (2010). Aerosol Light Extinction Measurements by Cavity Attenuation Phase Shift Spectroscopy (CAPS): Laboratory Validation and Field Development of a Compact Aerosol Extinction Monitor, *Aerosol Sci. Technol.* 44:428-435.

Modest, M.F. (2013). *Radiative Heat Transfer*, Third Edition, Academic Press.

Moosmüller, H., Arnott, W.P. (2003). Angular Truncation Errors in Integrating Nephelometry, *Rev. Sci. Instrum.* 74:3492-3501.

Moosmüller, H., Chakrabarty, R.K., and Arnott, W.P. (2009). Aerosol Light Absorption and Its Measurement: A Review, *J. Quantitative Spectroscopy & Radiative Transfer*, 110:844-878.

Onasch, T.B., Massoli, P., Kebabian, P.L., Hills, F.B., Bacon, F.W., Freedman, A. (2015). Single Scattering Albedo Monitor for Airborne Particulates, *Aerosol Sci. Technol.* 49:267-279.

Petzold, A., Ogren, J.A., Fiebig, M., Laj, P., Li, S.-M., et al. (2013). Recommendations for Reporting "Black Carbon" Measurements, Atmos. Chem. Phys. 13:8365-8379.

Qian, F., Ma, L., and Thompson, J.E. (2012) Modeling and Measurements of Angular Truncation for an Aerosol Albedometer. J. Euro. Opt. Soc. Rap. Public. 7-12021.

Shindell, D., Kuylenstierna, J.C.I., Vignati, E., van Dingenen, R., Amann, M., et al. (2012). Simultaneously Mitigating Near-Term Climate Change and Improving Human Health and Food Security, Science, 335:183-189.

Varma, R., Moosmüller, H., and Arnott, W.P. (2003). Toward and Ideal Integrating Nephelometer. Optics Lett. 28:1007-1009.

Wilker, E.H., Baccarelli, A., Suh, H., Vokonas, P., Wright, R.O., Schwartz, J. (2010). Black Carbon Exposures, Blood Pressure, and Interactions with Single Nucleotide Polymorphisms in MicroRNA Processing Genes, *Environ. Health Perspect.* 118:943-948.

Zhao, W., Xu, X., Dong, M., Chen, W., Gu, X., et al. (2014). Development of a Cavity-Enhanced Aerosol Albedometer, *Atmos. Meas. Tech.* 7:2551-2566.